NANO LETTERS

Letter

pubs.acs.org/NanoLett

New Approach to Fully Ordered fct-FePt Nanoparticles for Much Enhanced Electrocatalysis in Acid

Qing Li,[†,∥] Liheng Wu,[†,∥] Gang Wu,[‡] Dong Su,[§] Haifeng Lv,[†] Sen Zhang,[†] Wenlei Zhu,[†] Anix Casimir,[‡] Huiyuan Zhu,[†] Adriana Mendoza-Garcia,[†] and Shouheng Sun*[,†]

[†]Department of Chemistry, Brown University, Providence, Rhode Island 02912, United States

[‡]Department of Chemical and Biological Engineering, University at Buffalo, the State University of New York, Buffalo, New York 14260, United States

[§]Center for Functional Nanomaterials, Brookhaven National Laboratory, Upton, New York 11973, United States

S *Supporting Information*

ABSTRACT: Fully ordered face-centered tetragonal (fct) FePt nanoparticles (NPs) are synthesized by thermal annealing of the MgO-coated dumbbell-like FePt-Fe_3O_4 NPs followed by acid washing to remove MgO. These fct-FePt NPs show strong ferromagnetism with room temperature coercivity reaching 33 kOe. They serve as a robust electrocatalyst for the oxygen reduction reaction (ORR) in 0.1 M $HClO_4$ and hydrogen evolution reaction (HER) in 0.5 M H_2SO_4 with much enhanced activity (the most active fct-structured alloy NP catalyst ever reported) and stability (no obvious Fe loss and NP degradation after 20 000 cycles between 0.6 and 1.0 V (vs RHE)). Our work demonstrates a reliable approach to FePt NPs with much improved fct-ordering and catalytic efficiency for ORR and HER.

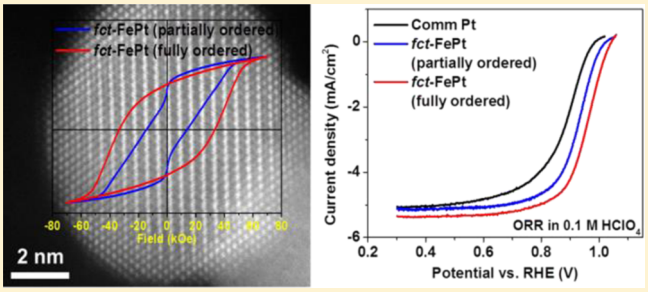

KEYWORDS: *face-centered tetragonal structure, nanoparticles, electrocatalysis, oxygen reduction, hydrogen evolution*

Developing highly efficient catalysts for oxygen reduction reaction (ORR) and hydrogen evolution reaction (HER) in acid media is crucial for promoting electrochemical energy conversion in fuel cells and for facile production of clean fuel, hydrogen, via water splitting. Nanostructured platinum (Pt), especially Pt nanoparticles (NPs), have been selected either as a model system for understanding electrochemical reduction mechanism or as a practical catalyst to achieve high-enough energy conversion efficiency in electrochemical devices. Recent studies have been focusing heavily on Pt-based alloy NPs, hoping to further enhance Pt catalysis and to lower Pt loadings. As a result, these alloy NPs can now be synthesized with the desired dimension controls and their catalytic activities are tuned not only by NP sizes/compositions/shapes[1−8] but also by the core/shell structure in which Pt alloys serve as a shell.[9−15] Alternatively, a Pt catalyst can be embedded in an ionic liquid medium to improve its ORR catalysis.[3,16] Despite this progress, there is still no definite answer on what form of the catalyst can yield maximal activity with much improved durability in the acidic electrochemical reduction conditions.

In the effort of searching for the most active form of Pt, a new strategy of controlling Pt alloy structure attracts much attention. For example, the FePt alloy NPs prepared for ORR studies often have a solid solution structure in which Fe and Pt occupy randomly the face-centered cubic (fcc) lattice. For notation convenience, these NPs are referred to as fcc-FePt NPs. With the proper composition control, the fcc structure can be converted to chemically ordered face-centered tetragonal (fct) structure. Earlier studies have indicated that the fct-FePt is not only magnetically hard,[17] but also chemically robust against Fe leaching in acid[18] and catalytically more active for ORR than the fcc-FePt.[18,19] This structure-induced catalytic enhancement is also observed in CoPt[20] and CuPt[21] NP systems. In general, high temperature annealing (>500 °C) is required to convert the fcc structure to the fct one, which causes NP to aggregate/sinter.[22,23] Although NPs coated with a layer of robust oxide (such as MgO[18,24] and SiO_2[25,26]) or supported on carbon can be stabilized against aggregation/sintering, the protection also limits atom mobility within the NP structure, making it more difficult for structure transformation from fcc to fct. As a result, partially ordered fct-FePt NPs are often obtained and studied,[18,27] compromising the benefit of fct-structure effect on ORR. Here, we report a new strategy to improve fcc−fct transition and demonstrate that the increase in fct-ordering in the FePt structure is indeed an effective way of enhancing NP catalytic efficiency for electrochemical reduction reactions, the fully ordered fct-FePt NPs serve as a robust catalyst for both ORR and HER.

Received: December 23, 2014
Revised: February 10, 2015

DOI: 10.1021/acs.nanolett.5b00320
Nano Lett. XXXX, XXX, XXX−XXX

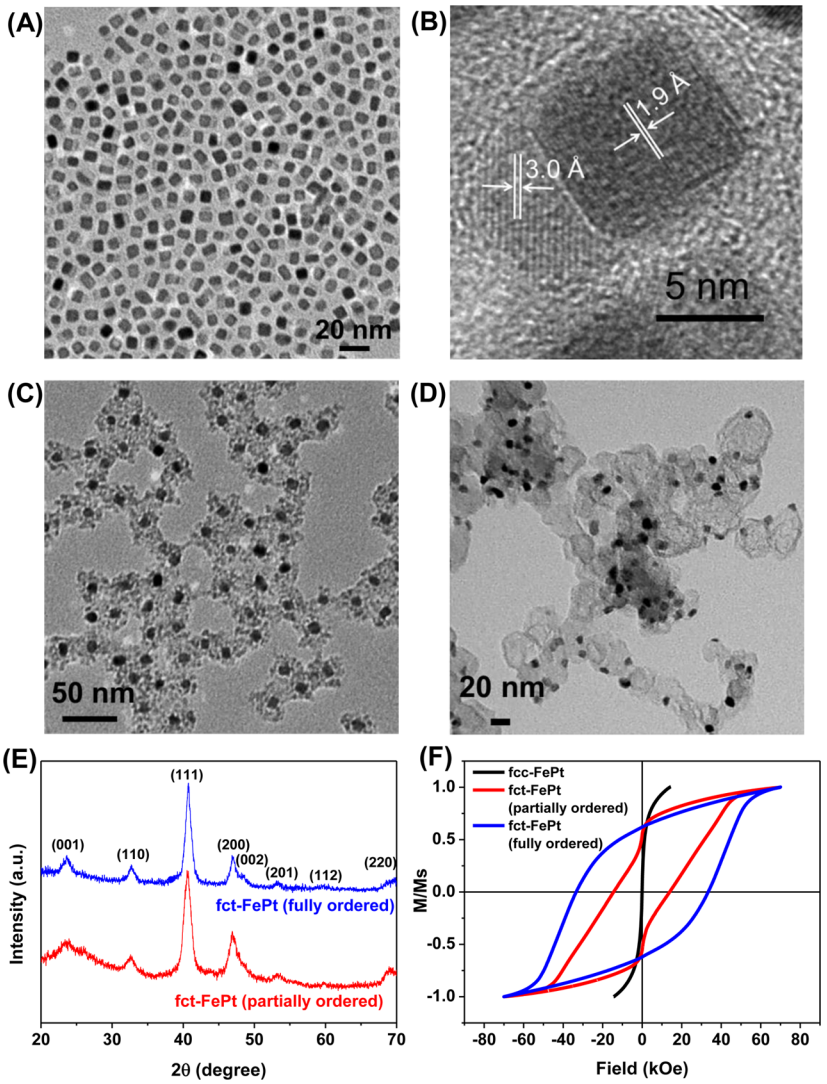

Figure 1. (A) TEM and (B) HR-TEM images of the as-synthesized dumbbell fcc-FePt-Fe_3O_4 NPs. (C) TEM image of the fcc-FePt-Fe_3O_4/MgO NPs. (D) TEM image of the C-fct-FePt (fully ordered) after thermal annealing at 700 °C under Ar + 5% H_2 for 6 h and acid wash. (E) XRD patterns of the fully and partially ordered fct-FePt NPs. (F) Hysteresis loops of the fcc-FePt and the fully and partially ordered fct-FePt NPs.

In our synthesis, the dumbbell-like fcc-FePt-Fe_3O_4 NPs were prepared by controlled decomposition of iron pentacarbonyl ($Fe(CO)_5$) and reduction of platinum acetylacetonate (Pt-$(acac)_2$) at temperatures 220 and 300 °C (Supporting Information). Here, 220 °C heating was used to form Pt-rich fcc-FePt NPs and 300 °C was for more Fe growth on the fcc-FePt. Upon air oxidation, dumbbell fcc-FePt-Fe_3O_4 NPs were obtained. In the process, the amount of $Fe(CO)_5$ was optimized so that the Fe/Pt composition in the as-synthesized dumbbell fcc-FePt-Fe_3O_4 NPs was at 52/48, as analyzed by inductively coupled plasma atomic emission spectroscopy (ICP-AES), to facilitate fcc−fct transition.[17] The dumbbell NPs were coated with MgO through thermal decomposition of magnesium(II) acetylacetonate in the presence of 1,2-tetradecanediol, oleic acid and oleylamine in benzyl ether at 300 °C (Supporting Information).[18] The fcc-FePt-Fe_3O_4/MgO NPs were then annealed at 700 °C under Ar + 5% H_2 to reduce Fe_3O_4 into Fe (to create O-vacancies) and to promote Fe, Pt diffusion into fully ordered fct-structure within the MgO enclosure. The MgO coating was removed by diluted nitric acid washing and the fct-FePt NPs were dispersed in ethanol and deposited on Ketjen carbon (Supporting Information) for further studies.

TEM images (Figure 1A,B) show that the as-synthesized dumbbell FePt-Fe_3O_4 NPs have an average size of 8.0 (±0.6)-3.9 (±0.3) nm and a lattice fringe spacing at 0.19 nm in the black FePt NP and at 0.30 nm in the gray Fe_3O_4 NP, corresponding to the lattice planes of fcc-FePt (200) and fcc-Fe_3O_4 (220), respectively. TEM image of the fcc-FePt-Fe_3O_4/MgO NPs (Figure 1C) shows that all NPs are covered by the MgO shell. Thanks to this protection, the annealed FePt NPs show no aggregation/sintering (Figure 1D and Supporting Information Figure S1). The average size of the annealed FePt NPs was measured to be 8.8 ± 0.5 nm. X-ray diffraction (XRD) patterns of the FePt NP powder were collected to characterize structure transition from fcc to fct upon thermal annealing. Supporting Information Figure S2 and Figure 1E shows the XRD patterns of the as-synthesized fcc-FePt-Fe_3O_4 and fct-FePt NPs after removing the MgO coating, respectively. The as-synthesized FePt-Fe_3O_4 shows typical fcc pattern as shown in Supporting Information Figure S2. After annealing in Ar + 5% H_2 at 700 °C for 1 h, the FePt NPs show the (001)/(110) peaks that are associated with the fct structure (Figure 1E). The

DOI: 10.1021/acs.nanolett.5b00320
Nano Lett. XXXX, XXX, XXX−XXX

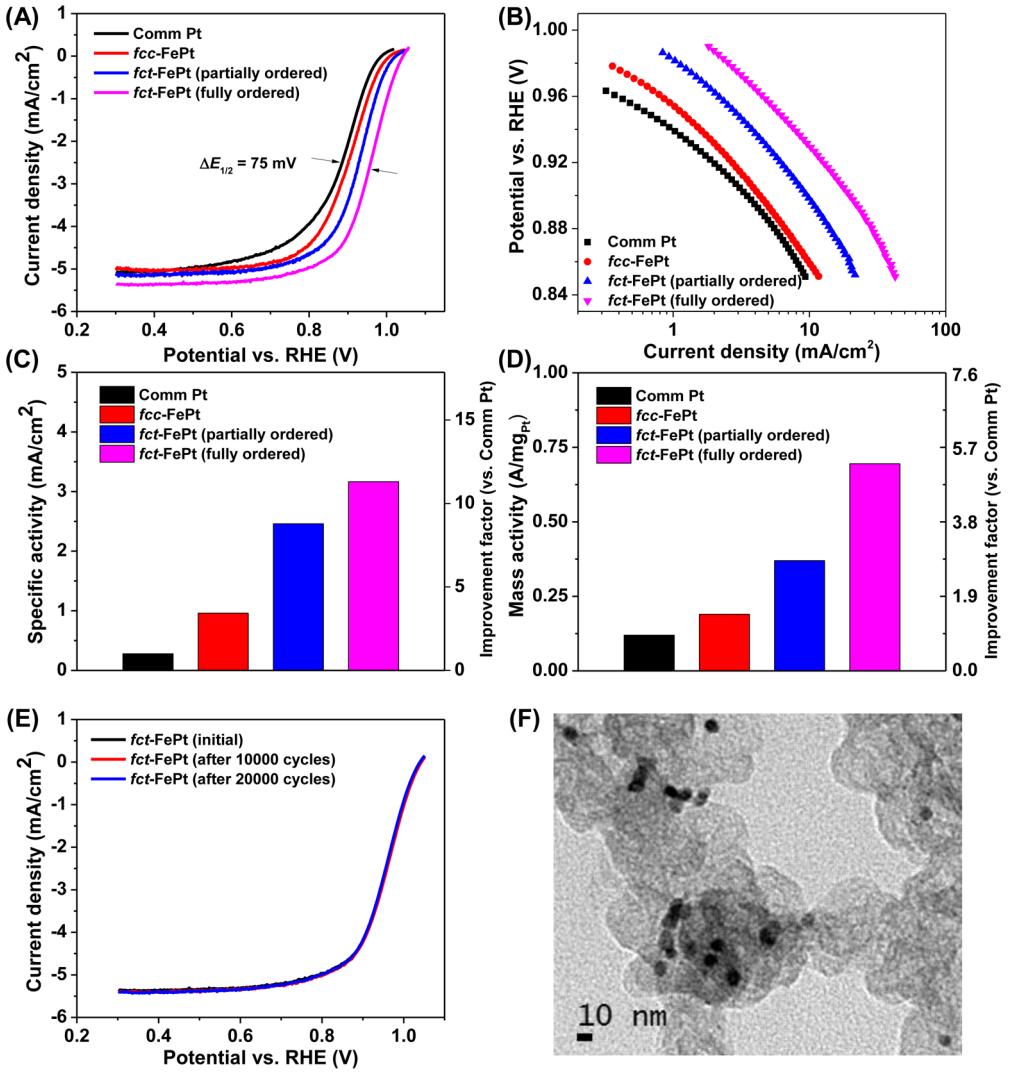

Figure 2. (A) ORR polarization curves of C-Pt, C-fcc-FePt, partially and fully ordered C-fct-FePt NPs in 0.1 M $HClO_4$ (rotating speed, 1600 rpm; scan rate, 10 mV/s). (B) Tafel plots for the ORR on different catalysts. (C) Specific activities of different catalysts at 0.9 V. (D) Mass activities of different catalysts at 0.9 V. (E) ORR polarization curves of the fully ordered fct-FePt NPs before and after potential scans between 0.6 and 1.0 V. (F) TEM image of the fully ordered fct-FePt NPs after 20 000 potential scans.

Fe, Pt ordering in the fct-structure is further improved by increasing the annealing time to 6 h, as indicated by much more visible (001)/(110) peaks. This fcc−fct structure transition is further supported by magnetic measurements. Different from the fcc-FePt NPs that are superparamagnetic at room temperature, the fct-FePt, due to the strong d electron interaction between Fe and Pt in the chemically ordered fct structure,[28,29] are strongly ferromagnetic (Figure 1F). Magnetically, a sub-10 nm fct-FePt with coercivitiy reaching 20 kOe (or 2 T) is considered to have good chemical ordering.[30] The 1 h annealed FePt NPs show a two-phase hysteresis behavior with the coercivity at 14 kOe. The soft behavior comes most likely from the existing Fe phase. These FePt NPs are denoted as "partially ordered" fct-FePt NPs. As a comparison, the 6 h annealed FePt NPs have a single-phase loop and their coercivity reaches 33 kOe (or 3.3 T). This is a very large magnetic coercivity value for the sub-10 nm NPs,[24−26,31,32] further confirming that the long time annealing does result in much higher degree of chemical ordering within the FePt structure. These FePt NPs are denoted as "fully ordered" fct-FePt.

The high degree of fct-ordering between Fe and Pt in FePt tends to stabilize Fe in FePt against Fe leaching in an acid solution. For example, when suspended in a 0.5 M nitric acid for 1 h, the fully ordered fct-FePt NPs showed a very small Fe/Pt composition change from 52/48 to 50/50, but the partially ordered fct-FePt NPs had their Fe/Pt composition decreased to 41/59. Clearly, the Fe layer sandwiched by two Pt layers in the fct-FePt is greatly stabilized by strong d-orbital interactions between Fe and Pt.

To evaluate the fct-FePt NP catalysis for ORR, the carbon-supported catalyst was suspended in deionized water + isopropanol + 5% Nafion and deposited on glassy carbon rotating disk electrode (GC-RDE). The commercial Pt and the fcc-FePt NPs were also prepared and studied similarly as the controls (Figure S3 in Supporting Information). The electrode was subject to 200 cycles of potential scans between 0.05 and 1.3 V (vs RHE) in the N_2-saturated 0.1 M $HClO_4$ to obtain a stable current−potential curve. The electrochemically active surface area (ECASA) of the catalysts was calculated by integrating the hydrogen underpotential desorption (H_{upd}) peaks of their cyclic voltammograms (CVs) (Figure S4 and

DOI: 10.1021/acs.nanolett.5b00320
Nano Lett. XXXX, XXX, XXX−XXX

Supporting Information). ORR measurements were performed in O_2-saturated 0.1 M $HClO_4$ solution at room temperature. Figure 2A shows the ORR polarization curves for the fully and partially ordered fct-FePt NPs, fcc-FePt NPs, and commercial Pt. The polarization curves display the diffusion-limiting current region from ca. 0.3 to 0.8 V and the mixed kinetic-diffusion control region between ca. 0.8 and 1.0 V. The activity, as measured by the ORR onset and half-wave potentials ($E_{1/2}$) in the RDE polarization plots, increases in the following order: commercial Pt < fcc-FePt < partially ordered fct-FePt < fully ordered fct-FePt. The $E_{1/2}$ of the ORR on the commercial Pt is 0.883 V. Upon the Pt alloying with Fe to form fcc-FePt NPs, the $E_{1/2}$ value is positively shifted to 0.890 V, which is consistent with the Fe enhancement effect on Pt.[1] After fcc−fct transition, $E_{1/2}$'s of the partially ordered fct-FePt and the fully ordered fct-FePt NPs are further improved to 0.927 and 0.958 V, respectively. This 0.958 V is the most positive value obtained on ORR catalysis by the fct-MPt NPs tested in the similar conditions,[13,20,21] demonstrating the dramatic catalytic enhancement effect of the fully ordered fct-structure on ORR.

Figure 2B is the Tafel plots of the catalysts studied. All catalysts exhibit slopes of ca. −120 mV/dec at high overpotentials and ca. −60 mV/dec at low overpotentials, suggesting that the ORR rate-determining steps involve the migration of reaction intermediates and charge transfer, respectively.[33] The kinetic current density (j_k) was calculated from the ORR polarization curve according to the Koutecky−Levich eq (Supporting Information) and was further used to obtain mass activity (Pt utilization) and specific activity (intrinsic activity of Pt), as shown in Figure 2C and D. The specific and mass activities of the fully ordered fct-FePt NPs reach 3.16 mA/cm^2 and 0.69 A/mg$_{Pt}$, respectively, at 0.9 V, which are larger than those from the commercial Pt we tested in this work (0.28 mA/cm^2 and 0.13 A/mg$_{Pt}$) and from other fct-MPt NPs reported previously.[13,20,21] The H_2O_2 content in ORR catalyzed by the fully ordered fct-FePt was measured (by rotating ring/disk electrode) to be ∼1% (Supporting Information Figure S5), further attesting the high selectivity of these FePt NPs on catalyzing ORR via a four-electron process.

The fully ordered fct-FePt NPs also showed remarkable durability in the ORR test condition. Accelerated durability tests (ADT) of the catalysts were conducted by cycling the potential between 0.6 and 1.0 V in an O_2-saturated 0.1 M $HClO_4$ at room temperature, which is close to the typical potential range at fuel cell cathodes. For the Pt and fcc-FePt catalysts, 5000 cycles caused $E_{1/2}$ a negative shift of ∼60 mV (Supporting Information Figure S6) and ∼80 mV (Supporting Information Figure S7), respectively. The stability of the partially ordered fct-FePt was much improved, showing only slight performance loss after 10 000 cycles (Supporting Information Figure S8). The fully ordered fct-FePt NPs were the most durable catalyst, showing no obvious performance loss (Figure 2E), no NP morphology changes (Figure 2F), and very small Fe/Pt composition decrease from 50/50 to 47/53 after 20 000 potential cycles. As a comparison, for the partially ordered fct-FePt NPs reported previously, their Fe/Pt composition decreases from 50/50 to 26/74 after only 300 potential cycles.[27]

To evidence the NP stability, we characterized the fully ordered fct-FePt NPs after 20000 potential cycles by aberration-corrected high-angle annular dark field scanning transmission electron microscopy (HAADF-STEM) and STEM-electron energy loss spectroscopy (STEM-EELS) (Figure 3 and Supporting Information Figure S9). The Fe/Pt ordering in the fct-FePt NP is clearly indicated by the high (Pt) and low (Fe) Z contrasts (Figure 3A). The alternating intensity profile shown in the HAADF-STEM image (Figure 3B) further confirms the Fe/Pt ordering within the fct-FePt NP. At the NP surface, a thin Pt layer of ∼0.6 nm (ca. 2−4 atomic layers) seems to exsit as shown in the STEM-EELS line scans and 2D elemental mapping image (Supporting Information Figure S9), but overall, the NP is dominated by the layered Fe/Pt structure, proving that the fully ordered fct-FePt NPs are stable in the ORR condition.

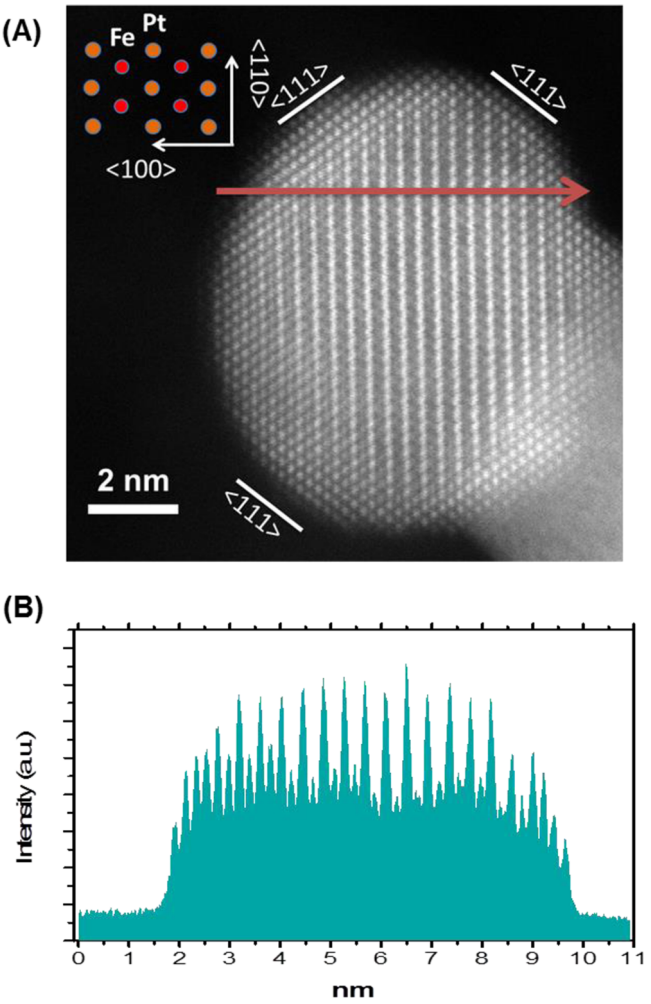

Figure 3. (A) HAADF-STEM image of a representative fully ordered fct-FePt NP after 20000 potential cycles. The arrow indicates the line scan position. An atomic model of the ordered structure is show at the inset. (B) Corresponding HAADF line profile across the line scan position shown in (A).

The fully ordered fct-FePt NP catalyst performed equally well in the H_2−air proton exchange membrane fuel cell (PEMFC) cathode under typical operating conditions.[34] The open circuit voltage (OCV) for the commercial Pt (0.959 V) is ca. 30 mV lower than that of the fct-FePt catalyst (0.989 V) at the same Pt loading (Supporting Information Figure S10). The fct-FePt shows ∼48% improved performance in the kinetically limited region than the Pt catalyst (0.378 A/cm^2 vs 0.256 A/cm^2 at 0.8 V). The maximum power density measured from the

DOI: 10.1021/acs.nanolett.5b00320
Nano Lett. XXXX, XXX, XXX−XXX

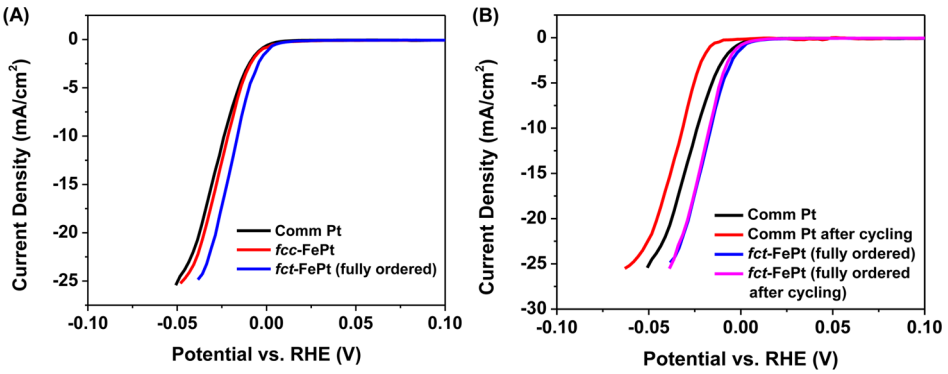

Figure 4. (A) HER polarization curves obtained with different catalysts as indicated. (B) HER activity of the commercial C−Pt and fully ordered C-fct-FePt before and after 10 000 potential cycling.

fct-FePt-based cells was 0.70 W/cm^2, higher than that from the Pt-based one (0.63 W/cm^2). These preliminary data indicate that the fully ordered fct-FePt is a new class of Pt-based catalyst with much desired activity and durability for practical applications in PEMFC.

The excellent ORR performance of the fully ordered fct-FePt NPs motivated us to study their catalysis for other electrochemical reduction reactions. Here, we chose to study HER, an important half-reaction in the electrochemical water splitting for hydrogen generation.[35] Although Pt has been the state-of-the-art catalyst used to catalyze HER,[3] it is still subject to acid etching and activity degradation. Figure 4A lists HER performance of the commercial Pt, fcc-FePt, and fully ordered fct-FePt in 0.5 M H_2SO_4, showing the activity increase in the order of Pt < fcc-FePt < fct-FePt. The fct-FePt NPs even exhibit higher activity than other Pt-based catalysts reported.[3,36] The catalyst durability was assessed by applying 10 000 potential sweeps between −0.3 and 0.9 V (Figure 4B). For the Pt catalyst, the potential cycling causes the obvious potential shift (~7 mV at 10 mA/cm^2). For the fct-FePt NPs, two polarization curves obtained before and after the cycling test nearly overlap. The tests prove that the fully ordered fct-FePt NPs are a class of new catalyst with efficiency much superior to any other Pt-based catalysts ever developed for HER.

In summary, this work reports a new approach to monodisperse fully ordered fct-FePt NPs via controlled annealing of MgO-coated dumbbell fcc-FePt-Fe_3O_4 NPs. In the synthesis, MgO functions as a protecting layer to prevent NPs from sintering in the high temperature annealing condition, Fe_3O_4 helps to create defects upon Fe_3O_4 reduction to Fe, and the dumbbell structure ensures the easy Fe/Pt diffusion to form fully ordered fct-structure. The fully ordered fct-FePt NPs are characterized by their much-enhanced ferromagnetism (room temperature coercivity reaching 33 kOe) and robust chemical stability against Fe etching in the strong acid solution. Compared with other fct-structured alloy NPs in the similar test conditions, the fully ordered fct-FePt NPs show the highest activity and longest durability in catalyzing ORR in 0.1 M $HClO_4$ and HER in H_2SO_4 without obvious Fe loss and NP degradation. The synthetic strategy demonstrated here is not limited to FePt, but can be extended to other Pt alloy NPs, such as CoPt NPs, and non-Pt alloy NPs, such as FePd and CuAu NPs, providing a versatile approach to fct-alloy NPs with much enhanced catalytic stability and activity for important energy conversion applications.

■ ASSOCIATED CONTENT

Supporting Information

Experimental details, TEM and HRTEM images of the partially ordered fct-FePt deposited on C, XRD pattern of the as-synthesized dumbbell fcc-FePt-Fe_3O_4 NPs, TEM images of 8 nm fcc-FePt NPs and C-fcc-FePt catalyst, CVs of the commercial Pt, fcc-FePt, partially ordered fct-FePt and fully ordered fct- FePt NPs in N_2-saturated 0.1 M $HClO_4$, H_2O_2 yield of fully-ordered fct-FePt NPs during ORR in 0.1 M $HClO_4$, ORR polarization curves of the commercial C-Pt before and after 5000 potential scans between 0.6 and 1.0 V, ORR polarization curves of the C-fcc-FePt NPs before and after 5000 potential scans between 0.6 and 1.0 V, ORR polarization curves of the partially ordered fct-FePt NPs before and after 10 000 potential scans between 0.6 and 1.0 V, AADF-STEM image of a representative fully-ordered fct-FePt NP after 20 000 potential cycles, STEM-EELS line scan, H_2−air fuel cell polarization plots recorded with various cathode catalysts. This material is available free of charge via the Internet at http://pubs.acs.org.

■ AUTHOR INFORMATION

Corresponding Author

*E-mail: ssun@brown.edu.

Author Contributions

[‖]These two authors contributed equally.

Notes

The authors declare no competing financial interest.

■ ACKNOWLEDGMENTS

This work was supported by the U.S. Army Research Laboratory and the U.S. Army Research Office under the Multi University Research Initiative (MURI, grant number W911NF-11-1-0353) on "Stress-Controlled Catalysis via Engineered Nanostructures". The electron microscopy work was partially carried out at the Center for Functional Nanomaterials, Brookhaven National Laboratory, which is supported by the U.S. Department of Energy (DOE), Office of Basic Energy Sciences, under Contract No. DE-AC02-98CH10886 and DE-SC-00112704.

■ REFERENCES

(1) Stamenkovic, V. R.; Mun, B. S.; Arenz, M.; Mayrhofer, K. J. J.; Lucas, C. A.; Wang, G. F.; Ross, P. N.; Markovic, N. M. *Nat. Mater.* **2007**, *6*, 241−247.

DOI: 10.1021/acs.nanolett.5b00320
Nano Lett. XXXX, XXX, XXX−XXX

(2) Guo, S. J.; Zhang, S.; Sun, S. H. *Angew. Chem., Int. Ed.* **2013**, *52*, 8526−8544.
(3) Chen, C.; Kang, Y. J.; Huo, Z. Y.; Zhu, Z. W.; Huang, W. Y.; Xin, H. L. L.; Snyder, J. D.; Li, D. G.; Herron, J. A.; Mavrikakis, M.; Chi, M. F.; More, K. L.; Li, Y. D.; Markovic, N. M.; Somorjai, G. A.; Yang, P. D.; Stamenkovic, V. R. *Science* **2014**, *343*, 1339−1343.
(4) Lim, B.; Jiang, M. J.; Camargo, P. H. C.; Cho, E. C.; Tao, J.; Lu, X. M.; Zhu, Y. M.; Xia, Y. N. *Science* **2009**, *324*, 1302−1305.
(5) Guo, S. J.; Li, D. G.; Zhu, H. Y.; Zhang, S.; Markovic, N. M.; Stamenkovic, V. R.; Sun, S. H. *Angew. Chem., Int. Ed.* **2013**, *52*, 3465−3468.
(6) Wu, J. B.; Qi, L.; You, H. J.; Gross, A.; Li, J.; Yang, H. *J. Am. Chem. Soc.* **2012**, *134*, 11880−11883.
(7) Choi, S. I.; Xie, S. F.; Shao, M. H.; Odell, J. H.; Lu, N.; Peng, H. C.; Protsailo, L.; Guerrero, S.; Park, J. H.; Xia, X. H.; Wang, J. G.; Kim, M. J.; Xia, Y. N. *Nano Lett.* **2013**, *13*, 3420−3425.
(8) Cui, C. H.; Gan, L.; Heggen, M.; Rudi, S.; Strasser, P. *Nat. Mater.* **2013**, *12*, 765−771.
(9) Zhang, J.; Lima, F. H. B.; Shao, M. H.; Sasaki, K.; Wang, J. X.; Hanson, J.; Adzic, R. R. *J. Phys. Chem. B* **2005**, *109*, 22701−22704.
(10) Wang, J. X.; Inada, H.; Wu, L. J.; Zhu, Y. M.; Choi, Y. M.; Liu, P.; Zhou, W. P.; Adzic, R. R. *J. Am. Chem. Soc.* **2009**, *131*, 17298−17302.
(11) Wang, C.; van der Vliet, D.; More, K. L.; Zaluzec, N. J.; Peng, S.; Sun, S. H.; Daimon, H.; Wang, G. F.; Greeley, J.; Pearson, J.; Paulikas, A. P.; Karapetrov, G.; Strmcnik, D.; Markovic, N. M.; Stamenkovic, V. R. *Nano Lett.* **2011**, *11*, 919−926.
(12) Sasaki, K.; Naohara, H.; Choi, Y. M.; Cai, Y.; Chen, W. F.; Liu, P.; Adzic, R. R. *Nat. Commun.* **2012**, *3*, 1115.
(13) Wang, G. W.; Huang, B.; Xiao, L.; Ren, Z. D.; Chen, H.; Wang, D. L.; Abruna, H. D.; Lu, J. T.; Zhuang, L. *J. Am. Chem. Soc.* **2014**, *136*, 9643−9649.
(14) Zhang, S.; Hao, Y. Z.; Su, D.; Doan-Nguyen, V. V. T.; Wu, Y. T.; Li, J.; Sun, S. H.; Murray, C. B. *J. Am. Chem. Soc.* **2014**, *136*, 15921−15924.
(15) Kang, Y. J.; Snyder, J.; Chi, M. F.; Li, D. G.; More, K. L.; Markovic, N. M.; Stamenkovic, V. R. *Nano Lett.* **2014**, *14*, 6361−6367.
(16) Snyder, J.; Fujita, T.; Chen, M. W.; Erlebacher, J. *Nat. Mater.* **2010**, *9*, 904−907.
(17) Sun, S. H.; Murray, C. B.; Weller, D.; Folks, L.; Moser, A. *Science* **2000**, *287*, 1989−1992.
(18) Kim, J.; Lee, Y.; Sun, S. H. *J. Am. Chem. Soc.* **2010**, *132*, 4996−4997.
(19) Prabhudev, S.; Bugnet, M.; Bock, C.; Botton, G. A. *ACS Nano* **2013**, *7*, 6103−6110.
(20) Wang, D. L.; Xin, H. L. L.; Hovden, R.; Wang, H. S.; Yu, Y. C.; Muller, D. A.; DiSalvo, F. J.; Abruna, H. D. *Nat. Mater.* **2013**, *12*, 81−87.
(21) Wang, D. L.; Yu, Y. C.; Xin, H. L. L.; Hovden, R.; Ercius, P.; Mundy, J. A.; Chen, H.; Richard, J. H.; Muller, D. A.; DiSalvo, F. J.; Abruna, H. D. *Nano Lett.* **2012**, *12*, 5230−5238.
(22) Elkins, K. E.; Vedantam, T. S.; Liu, J. P.; Zeng, H.; Sun, S. H.; Ding, Y.; Wang, Z. L. *Nano Lett.* **2003**, *3*, 1647−1649.
(23) Dai, Z. R.; Sun, S. H.; Wang, Z. L. *Nano Lett.* **2001**, *1*, 443−447.
(24) Kim, J. M.; Rong, C. B.; Liu, J. P.; Sun, S. H. *Adv. Mater.* **2009**, *21*, 906−909.
(25) Yamamoto, S.; Morimoto, Y.; Ono, T.; Takano, M. *Appl. Phys. Lett.* **2005**, *87*, 032503.
(26) Tamada, Y.; Yamamoto, S.; Takano, M.; Nasu, S.; Ono, T. *Appl. Phys. Lett.* **2007**, *90*, 162509.
(27) Zhang, S.; Zhang, X.; Jiang, G. M.; Zhu, H. Y.; Guo, S. J.; Su, D.; Lu, G.; Sun, S. H. *J. Am. Chem. Soc.* **2014**, *136*, 7734−7739.
(28) Brown, G.; Kraczek, B.; Janotti, A.; Schulthess, T. C.; Stocks, G. M.; Johnson, D. D. *Phys. Rev. B* **2003**, *68*, 052405.
(29) Burkert, T.; Eriksson, O.; Simak, S. I.; Ruban, A. V.; Sanyal, B.; Nordstrom, L.; Wills, J. M. *Phys. Rev. B* **2005**, *71*, 134411.
(30) Rong, C. B.; Li, D. R.; Nandwana, V.; Poudyal, N.; Ding, Y.; Wang, Z. L.; Zeng, H.; Liu, J. P. *Adv. Mater.* **2006**, *18*, 2984−2988.
(31) Kim, J.; Rong, C. B.; Lee, Y.; Liu, J. P.; Sun, S. H. *Chem. Mater.* **2008**, *20*, 7242−7245.
(32) Liu, F.; Zhu, J. H.; Yang, W. L.; Dong, Y. H.; Hou, Y. L.; Zhang, C. Z.; Yin, H.; Sun, S. H. *Angew. Chem., Int. Ed.* **2014**, *53*, 2176−2180.
(33) Coutanceau, C.; Croissant, M. J.; Napporn, T.; Lamy, C. *Electrochim. Acta* **2000**, *46*, 579−588.
(34) Wu, G.; More, K. L.; Johnston, C. M.; Zelenay, P. *Science* **2011**, *332*, 443−447.
(35) Karunadasa, H. I.; Montalvo, E.; Sun, Y. J.; Majda, M.; Long, J. R.; Chang, C. J. *Science* **2012**, *335*, 698−702.
(36) Greeley, J.; Jaramillo, T. F.; Bonde, J.; Chorkendorff, I. B.; Norskov, J. K. *Nat. Mater.* **2006**, *5*, 909−913.

DOI: 10.1021/acs.nanolett.5b00320
Nano Lett. XXXX, XXX, XXX−XXX